

# Quantum confinement effects on Mn-doped InAs nanocrystals: A first-principles study

J. T. Arantes,<sup>1,2</sup> G. M. Dalpian,<sup>2,\*</sup> and A. Fazzio<sup>1,2</sup>

<sup>1</sup>*Instituto de Física, Universidade de São Paulo, CP 66318, 05315-970 São Paulo, São Paulo, Brazil*

<sup>2</sup>*Centro de Ciências Naturais e Humanas, Universidade Federal do ABC, 09090-400, Santo André, São Paulo, Brazil*

(Received 19 July 2007; revised manuscript received 23 April 2008; published 1 July 2008)

We studied the effect of quantum confinement in Mn-doped InAs nanocrystals using theoretical methods. We observe that the stability of the impurities decreases with the size of the nanocrystals, making doping more difficult in small nanoparticles. Substitutional impurities are always more stable than interstitial ones, independent of the size of the nanocrystal. There is also a decrease in the energy difference between the high and low spin configurations, indicating that the critical temperature should decrease with the size of the nanoparticles, in agreement with experimental observations and in detriment to the development of functional spintronic devices with doped nanocrystals. Codoping with acceptors or saturating the nanocrystals with molecules that insert partially empty levels in the energy gap should be an efficient way to increase  $T_C$ .

DOI: 10.1103/PhysRevB.78.045402

PACS number(s): 71.20.Nr, 71.55.Eq, 73.22.-f, 75.50.Pp

## I. INTRODUCTION

With the advanced miniaturization of devices and the advent of nanotechnology, it is becoming important to understand the properties of materials in the nanometer scale.<sup>1,2</sup> Semiconductor nanocrystals are a class of materials that have already been highly studied. The observation and manipulation of these nanostructures can be done with great precision, although there are still many challenges to be overcome. *Ab initio* calculations can provide a good way to probe the properties of nanomaterials in a fast and efficient manner, giving directions for possible experiments and also explaining results that are not accessible through experiment. There are a few different ways to grow semiconductor nanocrystals. The most common are molecular-beam epitaxy (MBE), wet chemistry methods, and lithographic techniques. The growth through colloidal solutions is probably the cheapest method and the more suitable for mass production, although there are issues on how to functionalize the produced nanocrystals. Most of the current applications of these materials are related to luminescent properties that are very interesting and important although limited. It would be very important if one could use these materials to a wider array of applications such as energy, electronics, and computing.

An efficient way to functionalize semiconductors is through doping. This makes us believe that doping should also be an efficient way to functionalize semiconductor nanocrystals. Doping in nanocrystals through transition metals has already been achieved, showing intriguing behaviors. These diluted magnetic nanosemiconductors are also expected to be good candidates for spintronic applications. In order to achieve this, a good understanding of the properties of these materials is mandatory.<sup>3-7</sup> Although many authors claim to have successfully doped semiconductor nanocrystals, there are still a lot of discussions on whether the impurities are really incorporated into the nanocrystal or not.<sup>8</sup> In this paper, we will focus on  $(\text{In}_{1-x}\text{Mn}_x)\text{As}$  nanocrystals. These nanocrystals are easily grown by colloidal techniques<sup>9,10</sup> and also by epitaxial ways such as MBE,<sup>11-14</sup> providing a broad literature for comparison between the theoretical results obtained here and the experimental observations.

Although doping can be done in several different nanoparticles, there are some points that are still not understood in this kind of materials. For instance, ferromagnetism is usually not observed in small colloidal InAs nanocrystals<sup>10</sup> but is present in bulk InAs:Mn.<sup>15</sup> Ferromagnetism in other types of doped nanoparticles has already been observed.<sup>16</sup> It is also not clear if the impurities are inside the nanocrystal, at the surface of the nanocrystal, and if they are at substitutional or interstitial positions. In this work we present a systematic study of Mn-doped InAs nanoparticles, using an *ab initio* approach, based on density-functional theory. In particular, we look for the behavior of the structural, electronic, and magnetic properties of  $(\text{In}_{1-x}\text{Mn}_x)\text{As}$  nanocrystals as their size changes. From an electronic point of view, we can clearly observe an increased localization of the impurity levels as the size of the nanocrystal decreases, decreasing the interaction range between the impurities and consequently decreasing  $T_C$ .

## II. CALCULATION PROCEDURE

The calculations performed in this paper were done using total-energy *ab initio* methods based on spin-polarized density-functional theory within the generalized gradient approximation (GGA).<sup>17</sup> We used projector augmented wave (PAW) potentials<sup>18</sup> and a plane-wave expansion up to 440 eV as implemented in the VASP code.<sup>19</sup> Careful comparisons between PAW and pseudopotential methods show that both give very similar results for this kind of systems.<sup>20</sup> For bulk calculations we used a supercell with 64 In and As atoms with a  $(2 \times 2 \times 2)$  Monkhorst-Pack Brillouin-zone sampling. The calculated bulk lattice parameter is  $a = 6.149$  Å. For the InAs nanoparticles we used three supercells with different diameters. In all calculations the positions of all atoms in the supercell were allowed to relax until all the forces were smaller than 0.025 eV/Å. We have used a 12.0 Å vacuum space between the nanocrystal and its image to prevent spurious interactions. For the case of interstitial impurities, we used nanocrystals with different structures than for the substitutional impurities. For the interstitial case, the center of the nanocrystal is located at the tetrahedral interstitial site,

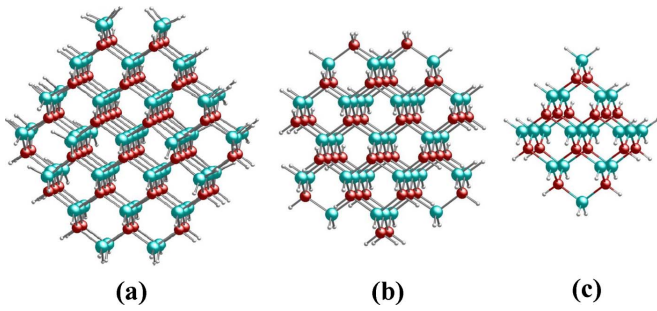


FIG. 1. (Color online) Relaxed nanocrystal structures representing diameters equal to (a) 2.0, (b) 1.7, and (c) 1.3 nm. The large spheres in cyan represent the In atoms, the medium spheres in red identify the As atoms, and the small spheres in gray are the hydrogen atoms. In a grayscale printing the cyan color appears as light gray representing the In atoms and the red one as dark gray for the As atoms.

whereas for the substitutional case the center is at the In site. This was done to save computer time and use better the symmetry of the nanocrystals.<sup>21</sup>

Our nanocrystals are obtained by cutting a spherical region of the bulk material. The three different sizes of nanocrystals were enough to give us in-depth information about the structural, electronic, and magnetic properties of the impurities in small nanocrystals. It is also possible to observe the chemical trends for the pure and doped nanocrystals as their size changes. Figure 1 shows the relaxed structure for the nanocrystals centered in an In atom. All our nanocrystals have one impurity each. The first nanocrystal has 247 atoms ( $\text{In}_{79}\text{As}_{68}\text{H}_{100}$ ), 2.0 nm of diameter, and manganese concentration of 1.26%. The second has 163 atoms ( $\text{In}_{43}\text{As}_{44}\text{H}_{76}$ ), 1.7 nm of diameter, and impurity concentration of 2.32%, and the last one has 71 atoms ( $\text{In}_{16}\text{As}_{19}\text{H}_{36}$ ), a diameter of 1.3 nm, and Mn concentration of 6.25%.

### III. RESULTS AND DISCUSSION

In order to analyze the electronic properties of these nanocrystals, we have saturated their surface with hydrogen atoms. The objective of the hydrogen atoms is to keep a local environment similar to an ideal tetrahedral structure. In real colloidal nanocrystals, the surface is usually passivated with organic molecules, such as trioctylphosphine oxide or butane. Theoretically, it is very difficult to simulate the surface of the nanocrystal as it really is, since the solutions are usually composed of large and complex molecules. With the hydrogen saturation, we can understand the effects of quantum confinement on the nanocrystal and of its internal structure, but there are problems in describing events occurring at the surface. In order to study the properties of the surface/interface of the nanocrystal, one should go to more sophisticated approaches.<sup>9,22,23</sup>

As the objective of the hydrogen atoms is just to passivate the surface of the nanocrystals, we also make use of hypothetical hydrogen atoms, with fractional charge. This is due to the fact that, depending on the atom that is saturated, either In or As, one has different complementary charges to

TABLE I. InAs nanoparticle energy gap as a function of nanoparticle diameter.

Diameter (nm)	Energy gap (eV)
1.3	2.83
1.7	1.97
2.0	1.56

satisfy the electron counting rule. The hydrogen atoms bonded to an In atom have valence charge of  $1.25e$  and the hydrogen atoms bonded to As atoms have valence charge of  $0.75e$ .

After relaxing all the atoms, we observe that the In-As bond distances are very similar to the bulk material. In the center of the nanocrystals the distances are usually larger than at the surface by  $\sim 1\%$ . There is no clear trend for the bond lengths as a function of the nanocrystal size.

The effect of quantum confinement in semiconductors is very well known. The energy gap of the material increases as confinement increases or, in the case of nanocrystals, as the size of the nanocrystal decreases. The change in the energy gap is usually proportional to the localization of the highest occupied molecular orbital (HOMO) and lowest unoccupied molecular orbital (LUMO). As the LUMO is more delocalized, it moves upward faster than the HOMO moves downward. Our calculated values for the energy gap of the isolated nanocrystals are shown in Table I.<sup>24</sup> In Fig. 2 it is also possible to observe the absolute change in the HOMO and LUMO for different nanocrystal sizes with respect to a deep valence level. In this figure it becomes clear the faster shift in energy of the LUMO.

The insertion of transition metals in bulk semiconductors leads to the inclusion of deep  $d$  levels either in the valence band or in the band gap of the semiconductor. If holes are inserted at the same time, such as in the case of Mn in InAs, the interaction between the impurities will be ferromagnetic (FM). This can be easily understood through the *band coupling model*, as described in Ref. 25. The search for high-temperature diluted magnetic semiconductors is a major challenge nowadays, and magnetic nanocrystals are potential candidates for this task.

In Mn-doped InAs, the  $d$  levels are inserted inside the valence band of the host. These levels hybridize with the host  $p$  levels with same symmetry, at the top of the valence band.<sup>25,26</sup> Figure 2 shows the projected density of states (PDOS) for the Mn  $d$  levels in different nanocrystals and for different positions of the impurities in the nanocrystals. The upper panels are for the majority-spin channels and the lower panels are for the minority spin. The eigenvalues were aligned through the lowest valence eigenvalue. Although the nanocrystals have different sizes and the atoms are in different positions, we can clearly observe that the impurity  $d$  levels are pinned in all of them,<sup>27</sup> except for the interstitial impurity [Fig. 2(f)], which has a different nature than the others. The alignment occurs for the *crystal-field split* levels inside the valence band and also for the *dangling-bond hybrid* levels near the Fermi energy. In the spin-up channel, there are  $d$

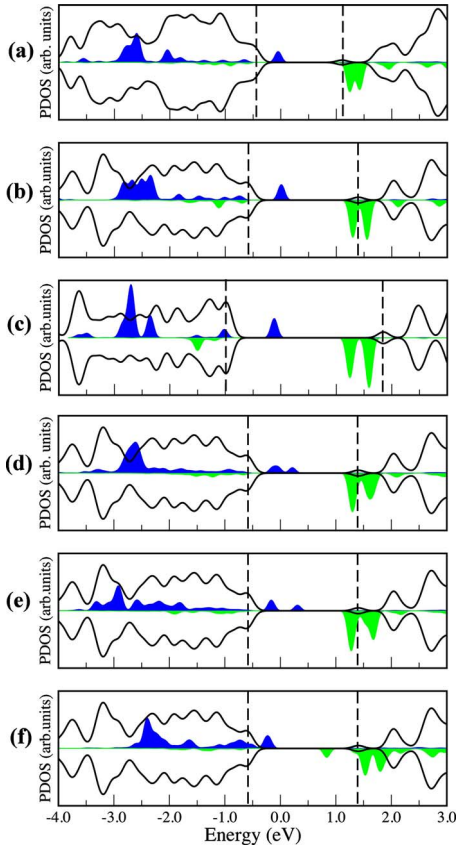


FIG. 2. (Color online) Projected density of states (PDOS) for the Mn  $d$  levels in different sizes of nanocrystals when the impurity is at and around the center of the nanocrystal. The nanoparticle diameters are equal to 2.0, 1.7, and 1.3 nm for (a), (b), and (c), respectively. The PDOSs for the substitutional impurity away from the center are shown in (d) and (e), while the interstitial case is shown in (f). The dashed line in the left (right) is the HOMO (LUMO) for the pure nanocrystal in its respective diameter. The majority spins are plotted in blue (black) and minority one in green (gray) for a color printing (grayscale printing).

levels at around  $-2.6$  eV that are present in all nanocrystals; this also occurs in the spin-down channel, where it is possible to observe the  $d$  levels at  $\sim 1.5$  eV. This confirms that deep levels are pinned energetically in semiconductor nanocrystals independent of their size,<sup>27</sup> in a similar way as deep transition-metal levels are pinned in different bulk semiconductors.<sup>28</sup>

Figure 3 shows the variation of the formation energy of an impurity inside the nanocrystals as their size changes. The formation energies for the substitutional ( $E_f^S$ ) and interstitial ( $E_f^I$ ) impurities were given by<sup>29</sup>

$$E_f^S = (E_{\text{def}} + \mu_{\text{In}}) - E_{\text{NC}} - \mu_{\text{Mn}}, \quad (1)$$

$$E_f^I = E_{\text{def}} - E_{\text{NC}} - \mu_{\text{Mn}}, \quad (2)$$

where  $E_{\text{def}}$  is the total energy of the supercell with the Mn atom at a substitutional or interstitial site.  $E_{\text{NC}}$  is the total energy of the nanocrystal without the Mn impurity.  $\mu_{\text{In}}$  and  $\mu_{\text{Mn}}$  are the In and Mn chemical potentials, respectively, in

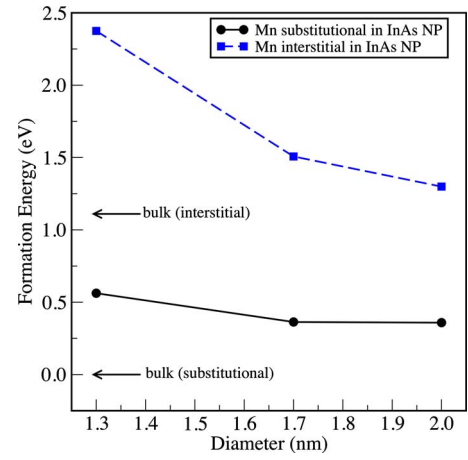


FIG. 3. (Color online) Mn formation energy, for both substitutional and interstitial impurities, as a function of the diameter of the nanocrystals. The reference was taken as the formation energy of the substitutional Mn in bulk InAs.

the In-rich regime. Although there are several possible positions for the impurities in the nanocrystal, we have focused on two different configurations: the In-substitutional site and a tetrahedral interstitial site where the Mn atom is first neighbor to four As atoms. Energetically, we observe that the impurities are more stable in the In-substitutional site independent of the size of the nanocrystal. The formation energy for the impurity in the interstitial site is 1.11 eV higher than the substitutional one for bulk InAs. Details about the procedure for calculating formation energies can be found elsewhere.<sup>30</sup> When the impurity is confined, the formation energy of both substitutional and interstitial sites increases as the size of the nanocrystal decreases. This is shown in Fig. 3, proving that doping of small nanocrystals should be very difficult.<sup>31</sup> The formation energy for the interstitial site increases faster than for the substitutional one. The comparison between interstitial and substitutional impurities in Fig. 3 is through absolute energies, showing that it is very unlikely that interstitial Mn impurities will occur in these materials.

Using the medium-size nanocrystal (diameter=1.7 nm) as a model, we investigate some positions for the substitutional Mn atom away from the nanoparticle center. We looked for these configurations because experimental results show that doping the center of a nanocrystal is very difficult.<sup>8,9</sup> We have not observed a clear trend between the stability of the impurity and its position inside the nanocrystal. The energy difference between the center of the nanoparticle and its first neighbor is 13 meV. Consequently, there is a very small tendency for the impurity to go to the surface of the nanocrystal. The difficulty in doping the center of the nanocrystal is probably related to the increased difficulty in doping the nanocrystal during the initial stages of its growth. The electronic structure for all the substitutional sites is very similar, as can be seen comparing Fig. 2(b) with Figs. 2(d) and 2(e).

Experimentally, from a magnetic perspective, it has been observed that Mn-doped InAs nanocrystals are not ferromagnetic.<sup>10</sup> This is a puzzling result, since this system has all the ingredients necessary to become a ferromagnetic

TABLE II. Variation of the total-energy difference between the low and high spin configurations for different nanocrystal sizes for Mn substitutional in In sites.

Diameter (nm)	$\Delta E^{\text{AFM-FM}}$ (meV)
Bulk	272
2.0	123
1.7	85
1.3	83

semiconductor: impurity  $d$  levels and the presence of holes. Up to now, this result has not been well explained. One option would be that the impurities might be located at interstitial sites, as occurs in many bulk samples. This should not be the case here since we observed that the formation energy of interstitial impurities increases very fast as the nanoparticle size decreases. Consequently the ratio between the population of interstitial and substitutional impurities should decrease with nanoparticle size. To clarify this point, we studied the interaction between two Mn atoms inside the nanocrystal in order to find its more stable configuration.

When two Mn atoms are inserted, we can set two different configurations for their local moment: parallel or antiparallel. When the magnetic moments of the two impurities are parallel to each other, we have a high spin configuration (compare to FM), and when they are antiparallel, we simulate a low spin configuration [compare to antiferromagnetic (AFM)]. The energetically more stable configuration will tell us if this material should be ferromagnetic or not. In a first-order approximation, the value of the energy difference between these two configurations can give us hints about the Curie temperature of this material: the larger the energy difference, the larger the  $T_C$ . More accurate approaches exist in order to find the  $T_C$  of a diluted magnetic semiconductor, but this is not our objective here.

In Table II we show the energy difference between the AFM and FM configurations for different nanoparticle diameters. The two Mn atoms were initially set to be first neighbors in the In lattice with one impurity at the center of the nanocrystal. We can clearly observe that this energy difference increases with the size of the nanocrystal, indicating that  $T_C$  of this material should decrease for small particles. For bulk InAs we found  $\Delta E^{\text{AFM-FM}}=272$  meV, whereas for the small nanocrystal  $\Delta E^{\text{AFM-FM}}=83$  meV. This result can be understood by the increased localization of the Mn  $d$  levels in the gap as the size of the nanocrystals decreases,<sup>7</sup> as shown in Fig. 2. As there is a large component of the Mn  $d$  levels in the band gap, ferromagnetic interactions should be mediated by double exchange, as predicted by the band coupling model.<sup>25</sup> The deeper the hole level is in the gap, the more localized it will be and  $T_C$  will also be lower since the overlap between these levels is smaller. In order to achieve the percolation threshold in this case, one should have a larger concentration of impurities. This result is in agreement with the lack of ferromagnetism observed in experiments and can give us a clear reason for it.

For the medium-size nanocrystal ( $d=1.7$  Å), we also studied the interaction between two Mn atoms at different sites, away from the center of the nanocrystal. When the Mn-Mn distance is 8.44 Å, the AFM-FM energy difference is  $\Delta E^{\text{AFM-FM}}=58$  meV, while for a larger Mn-Mn distance (12.11 Å) the energy difference is almost zero, showing that there is basically no interaction between the Mn atoms. When both impurities are near to the surface,  $\Delta E^{\text{AFM-FM}}=48$  meV. This energy difference is smaller than the one calculated for the Mn-Mn interaction when one of the Mn atoms is at the center of the nanoparticle, indicating that surface effects may contribute to decrease the ferromagnetic interaction of the dopants. These results are similar to those found in other transition-metal doped nanostructures.<sup>30</sup>

A very efficient approach that is used to tune the properties of diluted magnetic semiconductors is the inclusion of donors or acceptors to change the Fermi energy of the material and increase  $T_C$ .<sup>7,32</sup> In order to observe this effect in doped nanocrystals, we inserted a hole into the 87-atom nanocrystal by removing one electron from it. Ideally, this is equivalent to insert an acceptor into the nanocrystal. Nanomaterials have more degrees of freedom to insert holes into it: while in bulk this is done by doping with an element that has fewer electrons than the host, in nanocrystals it also may happen by functionalizing the surface of the nanocrystal. If one adsorbs a molecule that inserts empty levels into the energy gap of the nanocrystal, it will have the same effect as an acceptor impurity.

In our ideal calculations, the inclusion of a hole leads to an increase in the stability of the FM phase. The energy difference between the FM and AFM configurations increased from 85 to 182 meV. This is a very large increase and could lead to the successful observation of ferromagnetism in this kind of diluted magnetic nanosemiconductor.

#### IV. CONCLUSION

In summary, we have clearly demonstrated that the exchange interaction between magnetic impurities in semiconductor nanocrystals is weaker than in bulk. This should decrease the Curie temperature of this material, making it not suitable for spintronic applications. This weaker interaction occurs due to the increased localization of the hole levels in the band gap of the material. We show that deep levels are pinned energetically independent of nanocrystal size in nanostructures, also making doping of these nanocrystals more difficult. Hole doping of these nanocrystals should increase its  $T_C$  and maybe lead to the observation of room-temperature ferromagnetism.

#### ACKNOWLEDGMENTS

We thank Euclides Marega Júnior for useful discussions. Financial support from Brazilian agencies FAPESP and CNPq is gratefully acknowledged. Part of the calculations were performed at the computational facilities of the Centro Nacional de Processamento de Alto Desempenho (CENAPAD-Campinas/SP).

\*gustavo.dalpian@ufabc.edu.br

- <sup>1</sup>Y. Yin and A. P. Alivisatos, *Nature (London)* **437**, 664 (2005).
- <sup>2</sup>X. Peng, *Adv. Mater. (Weinheim, Ger.)* **15**, 459 (2003).
- <sup>3</sup>R. N. Bhargava, D. Gallagher, X. Hong, and A. Nurmikko, *Phys. Rev. Lett.* **72**, 416 (1994).
- <sup>4</sup>A. P. Alivisatos, *Science* **271**, 933 (1996).
- <sup>5</sup>D. J. Norris, N. Yao, F. T. Charnock, and T. A. Kennedy, *Nano Lett.* **1**, 3 (2001).
- <sup>6</sup>K. M. Hanif, R. W. Meulenberg, and G. F. Strouse, *J. Am. Chem. Soc.* **124**, 11495 (2002).
- <sup>7</sup>X. Huang, A. Makmal, J. R. Chelikowsky, and L. Kronik, *Phys. Rev. Lett.* **94**, 236801 (2005).
- <sup>8</sup>P. I. Archer, S. A. Santangelo, and D. R. Gamelin, *Nano Lett.* **7**, 1037 (2007).
- <sup>9</sup>S. C. Erwin, L. Zu, M. I. Haftel, A. L. Efros, T. A. Kennedy, and D. J. Norris, *Nature (London)* **436**, 91 (2005).
- <sup>10</sup>C. A. Stowell, R. J. Wiacek, A. E. Saunders, and B. A. Korgel, *Nano Lett.* **3**, 1441 (2003).
- <sup>11</sup>H. C. Jeon, Y. S. Jeong, T. W. Kang, T. W. Kim, K. Jae Chung, K. J. Chung, W. Jhe, and S. A. Song, *Adv. Mater. (Weinheim, Ger.)* **14**, 1725 (2002).
- <sup>12</sup>Y. F. Chen, W. N. Lee, J. H. Huang, T. S. Chin, R. T. Huang, F. R. Chen, J. J. Kai, K. Aravind, I. N. Lin, and H. C. Ku, *J. Vac. Sci. Technol. B* **23**, 1376 (2005).
- <sup>13</sup>H. Ofuchi, T. Kubo, M. Tabuchi, Y. Takeda, F. Matsukura, S. P. Guo, A. Shen, and H. Ohno, *J. Appl. Phys.* **89**, 66 (2001).
- <sup>14</sup>M. Holub, S. Chakrabarti, S. Fathpour, P. Bhattacharya, Y. Lei, and S. Ghosh, *Appl. Phys. Lett.* **85**, 973 (2004).
- <sup>15</sup>Y. L. Soo, S. W. Huang, Z. H. Ming, Y. H. Kao, H. MuneKata, and L. L. Chang, *Phys. Rev. B* **53**, 4905 (1996).
- <sup>16</sup>K. R. Kittilstved, W. K. Liu, and D. R. Gamelin, *Nat. Mater.* **5**, 291 (2006).
- <sup>17</sup>J. P. Perdew and Y. Wang, *Phys. Rev. B* **45**, 13244 (1992).
- <sup>18</sup>G. Kresse and D. Joubert, *Phys. Rev. B* **59**, 1758 (1999); P. E. Blöchl, *ibid.* **50**, 17953 (1994).
- <sup>19</sup>G. Kresse and J. Hafner, *Phys. Rev. B* **47**, 558 (1993).
- <sup>20</sup>A. J. R. da Silva, A. Fazzio, R. R. dos Santos, and L. E. Oliveira, *Phys. Rev. B* **72**, 125208 (2005).
- <sup>21</sup>G. M. Dalpian, M. L. Tiago, M. L. del Puerto, and J. R. Chelikowsky, *Nano Lett.* **6**, 501 (2006).
- <sup>22</sup>E. Rabani, *J. Chem. Phys.* **115**, 1493 (2001).
- <sup>23</sup>A. Puzder, A. J. Williamson, N. Zaitseva, G. Galli, L. Manna, and A. P. Alivisatos, *Nano Lett.* **4**, 2361 (2004).
- <sup>24</sup>First-principles density functional theory (DFT) calculations usually underestimate the band-gap energy of semiconductors.
- <sup>25</sup>G. M. Dalpian, S. H. Wei, X. G. Gong, A. J. R. da Silva, and A. Fazzio, *Solid State Commun.* **138**, 353 (2006).
- <sup>26</sup>T. M. Schmidt, P. Venezuela, J. T. Arantes, and A. Fazzio, *Phys. Rev. B* **73**, 235330 (2006).
- <sup>27</sup>N. S. Norberg, G. M. Dalpian, J. R. Chelikowsky, and D. R. Gamelin, *Nano Lett.* **6**, 2887 (2006).
- <sup>28</sup>M. J. Caldas, A. Fazzio, and A. Zunger, *Appl. Phys. Lett.* **45**, 671 (1984).
- <sup>29</sup>S.-H. Wei, *Comput. Mater. Sci.* **30**, 337 (2004).
- <sup>30</sup>J. T. Arantes, A. J. R. daSilva, and A. Fazzio, *Phys. Rev. B* **75**, 115113 (2007).
- <sup>31</sup>G. M. Dalpian and J. R. Chelikowsky, *Phys. Rev. Lett.* **96**, 226802 (2006).
- <sup>32</sup>T. Dietl, *Nat. Mater.* **5**, 673 (2006).